Experimental Performance Evaluation of Rx DSP-based Fiber-longitudinal Power Profile Estimation

Runa Kaneko
NTT Network Innovation Laboratories, NTT
1-1 Hikari-no-oka, Yokosuka
Kanagawa, Japan
runa.kaneko.sf@hco.ntt.co.jp

Takeo Sasai
NTT Network Innovation Laboratories, NTT
1-1 Hikari-no-oka, Yokosuka
Kanagawa, Japan
takeo.sasai.cp@hco.ntt.co.jp

Minami Takahashi
NTT Network Innovation Laboratories, NTT
1-1 Hikari-no-oka, Yokosuka
Kanagawa, Japan
minami.takahashi.xr@hco.ntt.co.jp

Etsushi Yamazaki
NTT Network Innovation Laboratories, NTT
1-1 Hikari-no-oka, Yokosuka
Kanagawa, Japan
etsushi.yamazaki.wk@hco.ntt.co.jp

Yoshiaki Kisaka
NTT Network Innovation Laboratories, NTT
1-1 Hikari-no-oka, Yokosuka
Kanagawa, Japan
yoshiaki.kisaka.dc@hco.ntt.co.jp

***Abstract*— The impact of fiber launch power, XPM, and number of samples on fiber-longitudinal power profile estimation was experimentally evaluated. By increasing samples, power profiles are clearly estimated even under an operational launch power and XPM.**

Keywords*— *Digital longitudinal monitoring, power profile estimation, correlation-based method, wavelength division multiplexing, fiber nonlinearity

I. Introduction

Various physical parameters in optical communication links need to be monitored to ensure stable and high-capacity transmission with less operational margins [1]. Numerous studies have been conducted to monitor the link parameters with the receiver (Rx) side digital signal processing (DSP), such as optical signal-to-noise ratio (OSNR) or fiber nonlinearity [2]. However, these approaches estimate the cumulative parameters of the entire link, which do not help in monitoring the distributed parameters. If longitudinally distributed parameters, such as the signal power profile along a fiber link, are available, we can identify anomalies in a link as well as estimate the quality of transmission (QoT) more accurately.

Accordingly, power profile estimation (PPE) methods [3]–[12] that visualize the signal power evolution in the fiber-longitudinal direction using only Rx DSP have been proposed. Compared with dedicated hardware devices such as an optical time domain reflectometer (OTDR), PPE has several significant advantages: (i) it can estimate the end-to-end characteristics of a link from a single coherent receiver, (ii) no additional instruments are required, and (iii) it can monitor other distributed parameters such as a chromatic dispersion (CD) map [6], [7], the gain spectrum of multiple amplifiers [7], [9], [10] misalignment of optical filters [7], and polarization dependent loss (PDL) [11].

However, the quantitative evaluation of PPE performance under experimental conditions has been limited. Since PPE uses fiber nonlinearity (nonlinear phase rotation) to estimate the signal power, PPE accuracy depends on (i) fiber launch power, (ii) the presence of wavelength division multiplexing (WDM), and (iii) number of signal samples used for PPE. Although PPE has been demonstrated under the WDM condition [3]–[5], [9], [10], the fiber launch power was far higher than the operational launch power, and the cross phase modulation (XPM) impact on PPE was not evaluated quantitatively. The dependency of these parameters is crucial for implementing PPE in practical networks.

In this study, we experimentally evaluate the impact of fiber launch power, XPM, and number of samples on PPE. Specifically, we investigate PPE accuracy under the following conditions: (i) 1-dBm (optimal launch power) or 6-dBm fiber launch powers of the PPE channel, (ii) single-channel or C-band transmission condition, and (iii) number of samples ranging from 10^4 to 10^7. The tested link was a 3-span × 50-km standard single-mode fiber (SSMF) link and the correlation-based method (CM) [12] was used for PPE. Results show that, by increasing the number of samples used for PPE, the estimated power profiles become clearly visible even in the presence of XPM and at a system operational fiber launch power. This result supports the implementation of PPE in practical networks.

II. Power Profile Estimation Method

As mentioned above, we used CM for PPE in this experiment. The optical signal propagating through the optical fiber is described by the nonlinear Schrödinger equation (NLSE);

$$\frac{\partial E}{\partial z} = \left(j\frac{\beta(z)}{2}\frac{\partial}{\partial^2 t} \right) E - j\gamma'(z)|E|^2 E, \qquad (1)$$

where

$$\gamma'(z) = \frac{8}{9}\gamma P(z) = \frac{8}{9}\gamma P(0)\exp\left(-\int_0^z \alpha(z')dz' \right). \qquad (2)$$

$\alpha(z)$, $\beta(z)$, γ, and $P(z)$ are the fiber loss, group velocity dispersion, nonlinear constant, and signal power profile, respectively, and $E = E(z,t)$ is the optical signal at position z and time t. For simplicity, we consider a single polarization transmission. Here, E is normalized to a power of 1. Instead, power variation due to fiber loss and amplification are dominated by $\gamma'(z)$. Therefore, if $\gamma'(z)$ can be estimated, $P(z)$ can also be estimated, assuming γ is constant. This can be regarded as inverse problem of finding the nonlinear

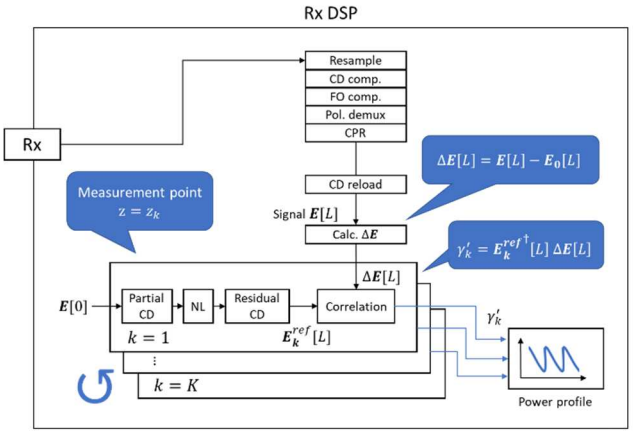

Fig. 1. DSP-function blocks and algorithms of PPE using CM.

coefficients of the NLSE from the boundary conditions (transmitted and received signals).

A. Correlation-Based Methods

The algorithm we used for CM is shown in Fig. 1. The power profile is estimated by performing the correlation between the received signal propagated over the actual transmission link and reference signal propagated over the digital twin link [8]. First, the transmitted signal $E[0]$ propagates along the transmission link and arrives at the receiver, and the CD, frequency offset (FO), polarization rotation, and carrier phase of the received signal $E[L]$ are compensated by the Rx DSP, where L represents the total transmission distance. After reloading the CD, the nonlinear perturbation term $\Delta E[L]$ is obtained from $E[L]$ as

$$\Delta \boldsymbol{E}[L] = \boldsymbol{E}[L] - \boldsymbol{E}_0[L] \tag{3}$$

$$\boldsymbol{E}_0[L] = \widehat{D}_{0L}\boldsymbol{E}[0] \tag{4}$$

where $\widehat{D_{0L}}$ is an operator that represents the CD corresponding to a distance from 0 to L km (assuming the homogeneous fiber type over the entire link). The reference signal is obtained using the simplified split-step method (SSM) in the digital domain from the transmitted signal $E[0]$. In a simplified SSM, the partial CD from 0 km to the measurement point $z = z_k$ $(k = 0, 1, \ldots, K-1)$is first applied to $E[0]$ as follows.

$$\boldsymbol{E}_0[z_k] = \widehat{D}_{0z_k}\boldsymbol{E}[0] \tag{5}$$

The following nonlinear operator is then applied at the measurement point $z = z_k$:

$$\boldsymbol{N}[z_k] = -j\boldsymbol{E}_0^{\dagger}[z_k] \odot \boldsymbol{E}_0[z_k] \odot \boldsymbol{E}_0[z_k], \tag{6}$$

where $\odot$ refers to element-wise multiplication. Finally, the residual CD from $z = z_k$ to $z = L$ is applied as follows.

$$\boldsymbol{E}_k^{\boldsymbol{ref}}[L] = \widehat{D}_{z_kL}\boldsymbol{N}[z_k] \tag{7}$$

Then the correlation of $\Delta \boldsymbol{E}[L]$ and $\boldsymbol{E}_{\boldsymbol{k}}^{\boldsymbol{ref}}[L]$ is taken as

$$\gamma'_k = \mathrm{Re}\left[\boldsymbol{E}_k^{\boldsymbol{ref}\dagger}[L]\Delta \boldsymbol{E}[L]\right] \tag{8}$$

By repeating this process for all measurement points z_k, the power profile of the entire fiber link is estimated.

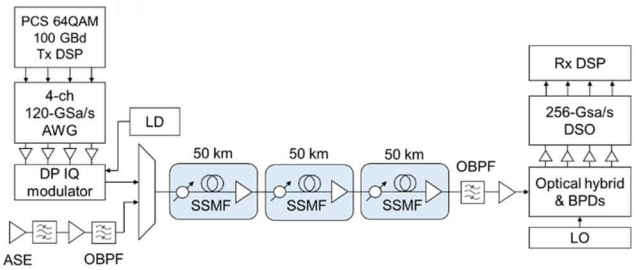

Fig. 2. Schematic diagram of experimental setup.

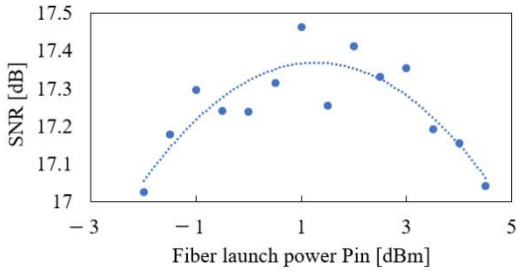

Fig. 3. SNR as a function of fiber launch power Pin.

III. Experimental Setup

The experimental setup is shown in Fig. 2. The transmitter consists of a 4-ch 120-GSa/s arbitrary waveform generator (AWG), driver amplifiers, a DP IQ modulator and laser diodes (LDs) that have a 40-kHz linewidth at 1547.31 nm. The receiver consists of a 90° optical hybrid, local oscillators (LOs), balanced photodetectors (BPDs), trans-impedance amplifiers (TIA), a 256-GSa/s digital storage oscilloscope (DSO), and Rx DSP. The signal for PPE (single-channel) is PCS 64QAM (H = 4.347, IR = 3.305, 21% FEC OH) 100 GBaud with a roll-off factor of 0.1, and its center frequency is 193.75 THz. The WDM channels are emulated using an ASE light source and covers the C-band (191–196.5 THz). The signal is transmitted through a 150-km 3-span SSMF link. The signal is adjusted by attenuators so that the fiber launch powers for all spans are constant.

We first examined the optimum fiber launch power of the transmission line by measuring the signal-to-noise (SNR) under the WDM condition. As shown in Fig. 3, the SNR is highest when the fiber launch power (Pin) is 1 dBm/ch. The WDM signal level was kept this level throughout the experiment. To investigate the impact of XPM and fiber launch power, we set the following four scenarios for the PPE channel. Again, Pin was kept constant for all spans.

(1) Pin = 1 dBm/ch, single-channel

(2) Pin = 1 dBm/ch, WDM condition

(3) Pin = 6 dBm/ch, single-channel

(4) Pin = 6 dBm/ch, WDM condition

For the number of samples used for PPE, we prepared five different conditions: 8.1×10^6, 1.6×10^6, 2.5×10^5, 7.5×10^4, and 2.5×10^4.

To quantify the PPE accuracy, we used the root-mean-square error (RMSE) between the estimated power profile and the reference power profile as a figure of merit.

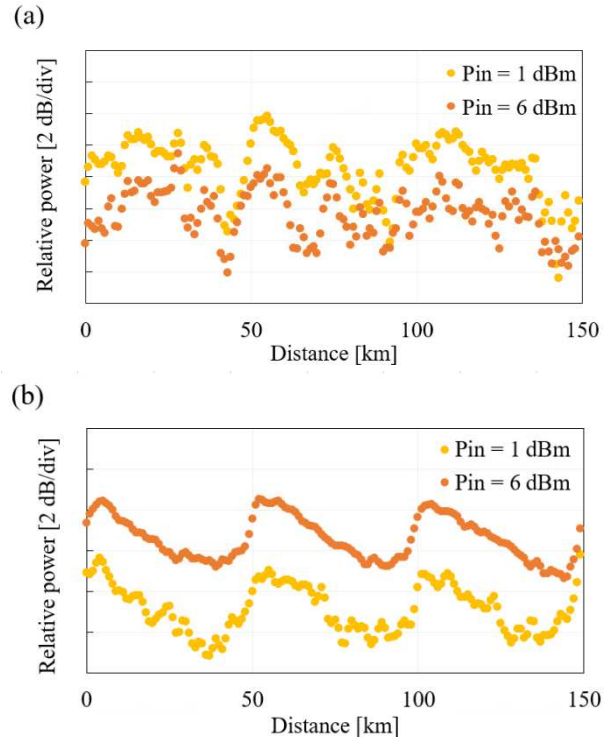

Fig. 4. Power profiles under WDM condition at Pin = 6 dBm and 1 dBm. Number of samples is (a) 8.1×10^6 and (b) 2.5×10^4.

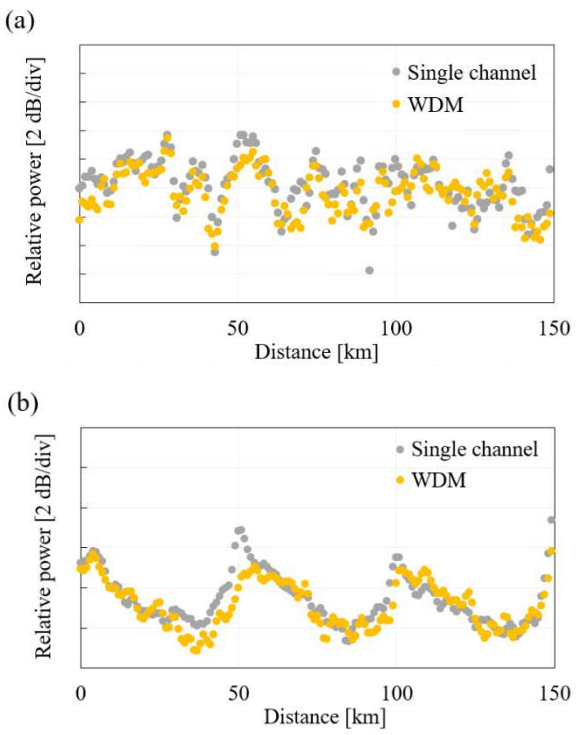

Fig. 5. Power profiles under single-channel and WDM conditions at Pin = 1 dBm. Number of samples is (a) 8.1×10^6 and (b) 2.5×10^4.

$$RMSE = \sqrt{\frac{1}{K}\sum_{k=0}^{K-1}\left|\gamma'_k - \gamma'^{ref}_k\right|^2} \quad (9)$$

where γ'^{ref}_k is the reference power profile when Pin is 6 dBm and the number of samples is largest (8.1×10^6 samples). The offset between the estimated power profile and reference was removed before the RMSE calculation using a least-squares method.

IV. Results and Discussion

Fig. 4 shows the estimated power profiles at Pin = 1 dBm (optimal Pin) and 6 dBm using (a) the minimum (2.5×10^4) and (b) maximum (8.1×10^6) number of samples. With 2.5×10^4 samples, the power profiles are noisy and the estimation fails regardless of Pin. Conversely, with 8.1×10^6 samples, the power profiles are clearly visible. Although Pin = 6 dBm offers clearer power profiles with less fluctuation, even Pin = 1 dBm still provides a sufficiently clear power profile.

Fig. 5 presents the estimated power profiles under single-channel and WDM conditions using (a) the minimum (2.5×10^4) and (b) maximum (8.1×10^6) number of samples. The power profiles are noisy with fewer samples but become clearly visible with more samples in both single-channel and WDM conditions. However, in the 1st and 2nd spans, there is a difference between power profiles for single-channel and WDM conditions, warranting further investigation.

Fig. 6 shows the relationship between RMSE (Eq. (9)) and the number of samples used for PPE. We discuss the results from three perspectives: (i) fiber launch power, (ii) presence or absence of adjacent channels, and (iii) the number of samples used for PPE. For (i), the RMSE is smaller at Pin = 6 dBm because PPE leverages the self-phase modulation (SPM), and high fiber launch power is preferrable for PPE. For (ii),

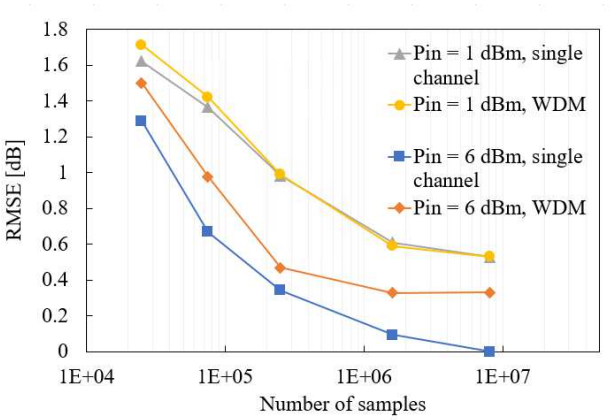

Fig. 6. Relationship between number of samples used for PPE and RMSE (Eq. (9)).

RMSE for single and WDM conditions does not differ at Pin = 6 dBm while the difference becomes significant at Pin = 1 dBm. This is because the SPM is more dominant than XPM at Pin = 6 dBm, stabilizing power profiles even in the WDM condition. However, at the system operational power (Pin = 1 dBm), the impact of XPM is non-negligible, causing the difference between single-channel and WDM conditions. For (iii), increasing the number of samples used for PPE reduces RMSE due to the averaging effect. Despite the impact of XPM persisting at increased samples, it is undeniable that the power profile is still clearly visible under system operational launch power and the presence of XPM, as shown in Fig. 5 (b). These results suggest that the PPE is feasible even during the system operation with optimal Pin and WDM conditions in a practical network.

V. Conclusion

In this work, we comprehensively evaluated the impact of (i) fiber launch power, (ii) XPM from adjacent channels, and (iii) number of samples on PPE. Findings indicate that increasing the samples for PPE allows for clear visibility of estimated power profiles, even under the presence of XPM, at 1-dBm (system operational) fiber launch power. This result supports the adoption of PPE in practical networks.

References

[1] Y. Pointurier, "Design of low-margin optical networks," in Journal of Optical Communications and Networking, vol. 9, no. 1, pp. A9-A17, Jan. 2017.

[2] Z. Wang, A. Yang, P. Guo, and P. He, "OSNR and nonlinear noise power estimation for optical fiber communication systems using LSTM based deep learning technique," Optics Express, vol. 26, no. 16, pp. 21346–21357, Aug. 2018.

[3] T. Tanimura, K. Tajima, S. Yoshida, S. Oda and T. Hoshida, "Experimental demonstration of a coherent receiver that visualizes longitudinal signal power profile over multiple spans out of its incoming signal," 45th European Conference on Optical Communication (ECOC), Dublin, Ireland, 2019, pp. 1-4.

[4] T. Tanimura, S. Yoshida, K. Tajima, S. Oda and T. Hoshida, "Fiber-Longitudinal Anomaly Position Identification Over Multi-Span Transmission Link Out of Receiver-end Signals," in Journal of Lightwave Technology, vol. 38, no. 9, pp. 2726-2733, 1 May1, 2020.

[5] T. Tanimura, S. Yoshida, K. Tajima, S. Oda and T. Hoshida, "Concept and implementation study of advanced DSP-based fiber-longitudinal optical power profile monitoring toward optical network tomography [Invited]," in Journal of Optical Communications and Networking, vol. 13, no. 10, pp. E132-E141, October 2021.

[6] T. Sasai, M. Nakamura, S. Okamoto, F. Hamaoka, S. Yamamoto, E. Yamazaki, A. Matsushita, H. Nishizawa and Y. Kisaka, "Simultaneous Detection of Anomaly Points and Fiber Types in Multi-Span Transmission Links Only by Receiver-Side Digital Signal Processing," 2020 Optical Fiber Communications Conference and Exhibition (OFC), San Diego, CA, USA, 2020, pp. 1-3.

[7] T. Sasai, M. Nakamura, E. Yamazaki, S. Yamamoto, H. Nishizawa and Y. Kisaka, "Digital Longitudinal Monitoring of Optical Fiber Communication Link," in Journal of Lightwave Technology, vol. 40, no. 8, pp. 2390-2408, 15 April15, 2022.

[8] T. Sasai, E. Yamazaki and Y. Kisaka, "Performance Limit of Fiber-Longitudinal Power Profile Estimation Methods," in Journal of Lightwave Technology, 2023, (early access).

[9] M. Sena, R. Emmerich, B. Shariati, C. Santos, A. Napoli, J. K. Fischer and R. Freund, "DSP-Based Link Tomography for Amplifier Gain Estimation and Anomaly Detection in C+L-Band Systems," in Journal of Lightwave Technology, vol. 40, no. 11, pp. 3395-3405, 1 June1, 2022.

[10] M. Sena, P. Hazarika, C. Santos, B. Correia, R. Emmerich, B. Shariati, A. Napoli, V. Curri, W. Forysiak, C. Schubert, J. K. Fischer and R. Freund, "Advanced DSP-Based Monitoring for Spatially Resolved and Wavelength-Dependent Amplifier Gain Estimation and Fault Location in C+L-Band Systems," in Journal of Lightwave Technology, vol. 41, no. 3, pp. 989-998, 1 Feb.1, 2023.

[11] M. Eto, K. Tajima, S. Yoshida, S. Oda and T. Hoshida, "Location-resolved PDL Monitoring with Rx-side Digital Signal Processing in Multi-span Optical Transmission System," 2022 Optical Fiber Communications Conference and Exhibition (OFC), San Diego, CA, USA, 2022, pp. 1-3.

[12] C. Hahn, J. Chang and Z. Jiang, "Localization of Reflection Induced Multi-Path-Interference Over Multi-Span Transmission Link by Receiver-side Digital Signal Processing," 2022 Optical Fiber Communications Conference and Exhibition (OFC), San Diego, CA, USA, 2022, pp. 1-3.